Journal of Solid Mechanics Vol. 16, No. 2 (2024) pp. 196-218
DOI: 10.60664/jsm.2024.3071783

Research Paper

Modal Data-Based Breathing Crack Localization in Beam-Column Structures Subjected to Axial and Transverse Harmonic Loading

P. Mirzaii [1], F. Akhlaghi [1], M. Bozorgnasab [1*], R. Taghipour [1], O. Yazdanpanah [2]

[1] *Department of Civil Engineering, University of Mazandaran, Babolsar, Iran*
[2] *Faculty of Engineering, Imam Khomeini University, Qazvin, Iran*

Received 24 July 2023; Received in revised form 11 August 2024; Accepted 6 September 2024

ABSTRACT

A sensitive modal data-based damage indicator is proposed to diagnose breathing cracks in beam-column structures subjected to axial load, as a percent of its critical value, and transverse harmonic load. The Newmark-Beta method is utilized to solve the equation of structural vibration, based on finite element method. The effect of Rayleigh-type damping is also examined. The indicator uses the modal deformations and their derivatives in healthy and damaged beam-column structures to identify the exact damage locations. The influence of some parameters such as noise effects and various axial loads on the efficiency of the method was also investigated. The results show the reliability of the approach in identifying the damage location for different scenarios, even in the presence of noise effect. Increasing the axial load, especially for values near to the critical load value, causes negative effects on the modal responses and their derivatives which are appropriately considered by the proposed index.

Keywords: Breathing crack; Damage identification; Beam-column structures; Harmonic load; Damage index.

1 INTRODUCTION

THE structural damage detection technique addresses the problem of how to locate and detect damage that occurred in a structure by using the observed changes in its dynamic and static characteristics. Many structural systems may experience some local damage during their lifetime. If the local damage is not identified timely, it may lead to a terrible outcome. During the last years, various researches were conducted to introduce appropriate damage identification approaches for beam structures. The cracks are usually shown through“open” or “breathing” crack models in vibration-based damage identification techniques. Open cracks are used for the case that the cracks are to

*Corresponding author. Tel.: +98 011 35302901.
E-mail address: m.bozorgnasab@umz.ac.ir (M. Bozorgnasab)

be considered open during structural vibration. This operation is usually adopted with the notched beams' functionin the case of substantial damages [1-20]. Breathing behavior is generally occurred in the case of fatigue cracks to consider the complexity resulted from nonlinear behavior. In fact, the breathing or closing crack model considers the vibration cycle of the structure, at which the crack edges come into or out of contact and result in sudden changes in the stiffness and dynamic structural responses [21-29]. The influence of damping on the nonlinearity level of the vibration response at the superharmonic resonance based on the finite element model of a beam with a closing crack was investigated by Bovsunovsky and Surace[30]. The goal of the work was to consider the change of damping due to the crack progress. A mathematical model of the beam with a closing crack based on the energy dissipated in the crack was developed. The model leads to predict the changes of damping of the cracked beam caused by the crack presence and compute its nonlinear behavior. A quantitative damage detection technique for a cantilever beam with a breathing crack using higher-order frequency response functions was developed by Chatterjee[31]. In this study, the bilinear restoring force was approximated by a Volterra series, and a nonlinear dynamic model of the cracked structure was proposed. The effect of crack severity on the response harmonic amplitudes was investigated, and a new procedure was suggested. Based on the results, the crack severity could be estimated through the measurement of the first and second harmonic amplitudes. An analytical-numerical method, based on the wavelet spectral finite element, was presented by Joglekar and Mitra[32] for studying the nonlinear interaction of flexural waves with a breathing crack present in a slender beam. A new damage index based on singular spectrum analysis for breathing crack detection and localization was proposed by Prawin et al.[33]. Their results show that the proposed breathing crack identification algorithm could be robust in the detection and identification of the particular location of the breathing crack present in the structure. Shariyat and Alipour [34] applied the differential transformation method for free vibration and modal stress analyses of two-directional functionally graded circular plates considering different elastic material properties and boundary conditions. Their results show the efficiency of the proposed approach.

The main objective of this study is to assess the efficiency of dynamic data for determining the location of breathing crack in beam-column structures, including axial load subjected to harmonic loading. For this purpose, a breathing crack in beam-column under harmonic loading was simulated using the finite element method. Rayleigh damping is assumed in the numerical simulation. Then, the equation of motion of structural vibration subjected to external harmonic force was solved through the Newmark-Beta approach. Consequently, an efficient damage indicator based on the healthy and damaged modal deformations and their derivatives are introduced to identify the exact damage locations in beam-column structures. It should be noted that the first and second derivatives of mode shapes were computed through the first and second order of central finite difference approximated formulas, respectively. The influence of many parameters such as Rayleigh damping, noise, and various axial load affecting the efficiency of the method was investigated. Numerical results demonstrate that the proposed damage index can well diagnose the locations of single and multiple damage cases having different characteristics. Moreover, the presented index for damage detection does not depend on the harmonic load position and its magnitude.

2. BREATHING DAMAGE (CRACK) MODELING IN A BEAM UNDER HARMONIC LOADING

The switching condition between closed and open behavior for the crack may occur in several applications. This condition leads to model the structure under consideration with a finite element, including a bilinear element matrix with a discontinuity [35-37]. The standard and undamaged element stiffness matrix K_u^e for a plane beam-column element with three degrees of freedom per node, collected in the vector U, according to Euler–Bernoulli beam-column element, is expressed as[38]:
Where

$$k_u^e=\begin{bmatrix} \frac{EA_u}{L_e} & 0 & 0 & -\frac{EA_u}{L_e} & 0 & 0 \\ 0 & q & \frac{k(1+c)}{L_e} & 0 & -q & \frac{k(1+c)}{L_e} \\ 0 & \frac{k(1+c)}{L_e} & k & 0 & -\frac{k(1+c)}{L_e} & kc \\ -\frac{EA_u}{L_e} & 0 & 0 & \frac{EA_u}{L_e} & 0 & 0 \\ 0 & -q & -\frac{k(1+c)}{L_e} & 0 & q & -\frac{k(1+c)}{L_e} \\ 0 & \frac{k(1+c)}{L_e} & kc & 0 & -\frac{k(1+c)}{L_e} & k \end{bmatrix},\quad U=\begin{Bmatrix} u_i \\ v_i \\ \theta_i \\ u_j \\ v_j \\ \theta_j \end{Bmatrix} \tag{1}$$

$$q=\frac{EI_u}{L_e^3}(ml)^2\left[\frac{\tan(\frac{ml}{2})}{\tan(\frac{ml}{2})-(\frac{ml}{2})}-1\right]$$

$$\frac{k(1+c)}{L_e}=\frac{EI_u}{L_e^2}\frac{(ml)^2}{2}\left[\frac{\tan(\frac{ml}{2})}{\tan(\frac{ml}{2})-(\frac{ml}{2})}\right]$$

$$kc=\frac{EI_u}{L_e}\frac{(ml)}{2}\left[\frac{(ml)\cos ec(ml)-1}{\tan(\frac{ml}{2})-(\frac{ml}{2})}\right]$$

$$k=\frac{EI_u}{L_e}\frac{(ml)}{2}\left[\frac{1-(ml)\cot g(ml)}{\tan(\frac{ml}{2})-(\frac{ml}{2})}\right] \tag{2}$$

$$ml=\pi\sqrt{\frac{P_a}{P_c}}\quad,\qquad P_c=\frac{\pi^2 EI_u}{L_e^2}$$

The presence of the breathing crack in the beam-column element considering the effect of the crack on the axial stiffness is modeled. The modeling process contains some changes in the element stiffness at the crack location. Assuming the crack initiation from the upper side of the beam-column element, the reduction in the stiffness matrix can be obtained as[33, 39]:

$$k_c=\begin{bmatrix} K_a & 0 & 0 & -K_a & 0 & 0 \\ & K_{22} & K_{23} & 0 & -K_{22} & K_{23} \\ & & K_{33} & 0 & -K_{23} & K_{36} \\ & & & K_a & 0 & 0 \\ & symm & & & K_{22} & -K_{23} \\ & & & & & K_{33} \end{bmatrix} \tag{3}$$

where the stiffness factors are considered as follows:

$$
\begin{aligned}
K_a &= \frac{E(A_u - A_c)}{L_e} \\
K_{22} &= \frac{\mu E}{L_u}\frac{12I_u}{L_e^2}, \\
K_{23} &= \frac{\mu E}{L_u}\frac{6I_u}{L_e}, \\
K_{33} &= \frac{\mu E}{L_u}4I_u, \\
K_{36} &= \frac{\mu E}{L_u}2I_u.
\end{aligned}
\tag{4}
$$

Where E is Young's modulus, L_e is the length of the element, A_u and $A_c = w(h - h_c)$ are healthy and cracked cross-sections, respectively, and P_c is the critical load. I_u and I_d are the healthy and damaged moments of inertia, respectively. h and w are the height and width of the intact beam-column element, and h_c is the crack depth. μ represents the non-dimensional flexural damage and has a value between 0 and 1 for the healthy and completely damaged section, respectively[33, 39]:

$$
\mu = \frac{I_u - I_d}{I_u}, \quad I_u = \frac{wh^3}{12}, \quad I_d = \frac{w(h-h_c)^3}{12}
\tag{5}
$$

The cracked element of the structure is initially assumed to be in the closed state under compression; the opening state occurs in tension condition through the rotations at the end nodes of the damaged element, i.e., rotations θ_i and θ_j for the damaged element "*ij*" with a breathing crack located between i and j)[30, 39, 40]. Consequently, the breathing behavior could be introduced through a damaged element matrix, k_d^e with a bilinear behavior as follows:

$$
k_d^e = k_u^e - H(\theta_i - \theta_j)k_c^e, \quad \begin{cases} H(\theta_i - \theta_j) = 1, & \theta_i > \theta_j \\ H(\theta_i - \theta_j) = 0, & \theta_i < \theta_j \end{cases}
\tag{6}
$$

Where H is the Heaviside step function and depends on the relative rotations between nodes i and j. As a matter of fact, the Heaviside function is used to model the bilinear stiffness behavior due to change from open to close state. So, the crack state is determined through evaluating the slope value of the response deformation at the damaged element nodes, i.e., i and j (see Figure 1)[30, 39].

In the case of more than one cracked element, the same procedure can be followed. The global stiffness matrix of the beam-column, K_d, is obtained by assembling the element stiffness matrices, including those of cracked elements.

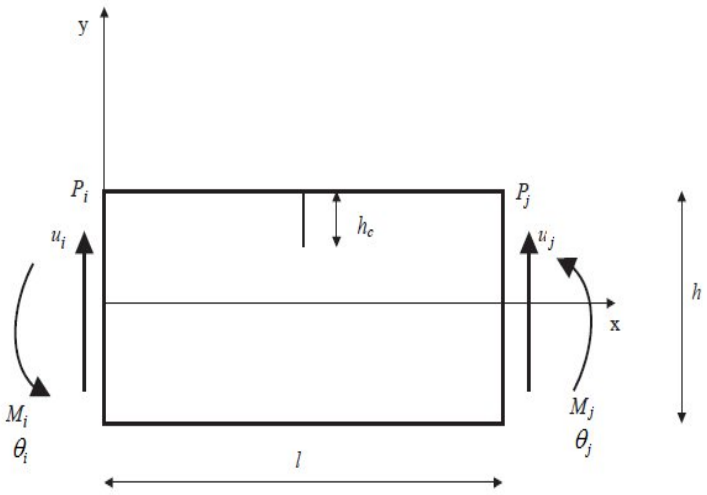

Fig. 1
The schematic view of breathing cracked element[30].

3. THE PROPOSED CRACK IDENTIFICATION METHOD

As mentioned previously, one of the nondestructive damage identification methods is the methods that are established based on dynamic data. One of the dynamic data that is sensitive to the occurred damage, is the deflection of the beam-column and its derivatives that are obtained through solving the dynamic equation. Change in dynamic response related to deflection of the structure before and after damage can be considered as a criterion for detecting the damage. Besides, its derivatives, such as slope and curvature, are more sensitive to the damage and can be considered for detecting the damage presence. For this purpose, an efficient indicator based on dynamic deflection and its derivatives was proposed. It is worth mentioning that Rayleigh damping is assumed for the numerical simulation, and damping ratios at the first and third mode periods of the beam-column structure are set to be 5% [41, 42]. Therefore, the deflection of the beam is obtained by solving the dynamic equation presented as follows[43] [44]:

$$M\ddot{u}(t) + C\dot{u}(t) + Ku(t) = F(t) \tag{7}$$

$$[K] = \sum_{e=1}^{N} \left[K^{(e)}\right] \tag{8}$$

$$[M] = \sum_{e=1}^{N} \left[M^{(e)}\right] \tag{9}$$

$$F(t) = p_0 \cos(t) \tag{10}$$

$$[C] = \alpha [M] + \beta [K] \tag{11}$$

Where *M*, *K*, *C,* and F are mass, stiffness, damping, and excitation force (harmonic load), respectively, and presented as follows[43, 44, 45]:
where *N* is the number of structural elements, and p_0 is the maximum value of $F(t)$. The values of α and β are the Rayleigh-type damping coefficients obtained based on the following equation[44, 45]:

$$\begin{cases} 2\zeta_1\omega_1 = \alpha + \beta\omega_1^2 \\ 2\zeta_3\omega_3 = \alpha + \beta\omega_3^2 \end{cases} \xrightarrow{\zeta_1 = \zeta_3 = \zeta} \begin{cases} \alpha = \dfrac{2\zeta}{\omega_1 + \omega_3}\omega_1\omega_3 \\ \beta = \dfrac{2\zeta}{\omega_1 + \omega_3} \end{cases} \tag{12}$$

Where, ζ is the damping ratio, and ω is the circular frequency. The indices in the above equation denote mode numbers, which depend on modal participation factors.

To solve Eq. (3.1) and consequently simulate the dynamic behavior of the undamaged and damaged structure, a step-by-step numerical procedure could be used. To this purpose, the well-known Newmark-Beta method is considered as follows[46]:

- Considering the initial deflection and initial velocity:

$$u = u_{0,}\ v_0 = \dot{u}_0 \tag{13}$$

- For constant-average acceleration method:

$$\gamma = 1/2,\ \ \beta = 1/4 \tag{14}$$

- Calculating $\ddot{u}$

$$\ddot{u} = \frac{p_0 - c\dot{u}_0 - ku_0}{m} \tag{15}$$

- Selecting time step Δt as[47-49]:

$$\Delta t = 0.1T_1 \tag{16}$$

$$\begin{aligned} &\hat{k} = k + \frac{\gamma}{\beta\Delta t}c + \frac{1}{\beta(\Delta t)^2}m \\ &a = \frac{1}{\beta\Delta t}m + \frac{\gamma}{\beta}c;\ \text{b} = \frac{1}{2\beta}m + \Delta t\left(\frac{\gamma}{2\beta} - 1\right)c \end{aligned} \tag{17}$$

- Calculating the following parameters for each time step *i:*

$$\begin{aligned} &\Delta\hat{p}_i = \Delta p_i + a\dot{u}_i + b\ddot{u}_i \\ &\Delta u_i = \frac{\Delta\hat{p}_i}{\hat{k}} \\ &\Delta\dot{u}_i = \frac{\gamma}{\beta\Delta t}\Delta u_i - \frac{\gamma}{\beta}\dot{u}_i + \Delta t\left(1 - \frac{\gamma}{2\beta}\right)\ddot{u}_i \\ &\Delta\ddot{u}_i = \frac{1}{\beta(\Delta t)^2}\Delta u_i - \frac{1}{\beta\Delta t}\dot{u}_i - \frac{1}{2\beta}\ddot{u}_i \\ &u_{i+1} = u_i + \Delta u_i, \dot{u}_{i+1} = \dot{u}_i + \Delta\dot{u}, \\ &\qquad \ddot{u}_{i+1} = \ddot{u}_i + \Delta\ddot{u} \end{aligned} \tag{18}$$

The above procedures are repeated for both the healthy and damaged structure. It should be noted that for modeling the damage, the moment of inertia is reduced (see Eq. (2.5)).

In this paper, the damaged identification of a beam-column structure is studied. The structure is modeled through a finite element procedure, using a MATLAB code[50]. The transverse deformations for the healthy and damaged structures are calculated for considered points; i.e., $u_{h(p)}$ and $u_{d(p)}$ for point, p on the healthy and damaged structure, respectively.

The deformations slope for the undamaged beam-columns, at any node p, $u'_{h(p)}$ can be calculated using the central finite difference approximation as:

$$u'_{h(p)} = \frac{u_{h(p+1)} - u_{h(p-1)}}{2L_e} \tag{19}$$

where L_e is the element length. For the damaged structure, the "h" is replaced by "d" in the above equation.

Moreover, the deformations curvature of the healthy structure can be achieved as:

$$u''_{h(p)} = \frac{u_{h(p-1)} - 2u_{h(p)} + u_{h(p+1)}}{L_e^{\,2}} \tag{20}$$

As stated before, for the damaged structure, the "h" is replaced by "d" in the above equation. For nodes located on the supports, the calculations of deformation derivatives could be conducted using forward or backward difference approximation.

It should be noted that it is assumed that the damage decreases the stiffness and therefore, can be simulated by a reduction in the moment of inertia (I) at the location of the damage.

Finally, using the dynamic responses (deformations, slope, and curvature of deformations) obtained previously, the harmonic load based indicator (HLBI) is proposed:

$$HLBI_p = \frac{\sum_{i=1}^{nm} \left\| \left[\left| u''_{d(p,i)} - u''_{h(p,i)} \right| \times \left(u_{d(p,i)} \right)^2 \right] - \left[\left(\left| u'_{d(p,i)} \right|^2 - \left| u'_{h(p,i)} \right|^2 \right) \times u_{h(p,i)} \right] \right\| \times \left(\left| u''_{d(p,i)} - u''_{h(p,i)} \right| \right)}{nm} \tag{21}$$

where, $HLBI_p$ is the indicator value for point *p (p=1,2,...,n+1), nm* is the number of iteration steps considered for the Newmark-Beta method.

Assuming a normal distribution for the values of the proposed indicator, the normalized form of the indicator can be calculated as follows:

$$nHLBI_{pi} = \left(\max \left[0, \left(\frac{HLBI_{pi} - mean(HLBI)}{std(HLBI)} \right) \right] \right) \tag{22}$$

Where mean (*HLBI*) and std (*HLBI*) represent the mean and standard deviation of ($HLBI_p$, $\mathrm{p} = 1, 2, ..., n+1$), respectively. It is worth noting that a borderline value of 0.05 is considered for $nHLBI_{pi}$, and lower values are not considered during the damage detection process.

To consider the noise effect, the below relation is used to apply ±*e* percent noise, i.e.,

$$Data_{Noise} = \left(1 + \frac{e}{100} \times (2 \times random - 1) \right) \times Data_{Noise-free} \tag{23}$$

Where, $Data_{Noise-free}$ and $Data_{Noise}$ are primary data(data without any noise) and noisy data, respectively. "random" is a random number between 0 and 1.

4. VALIDATION OF RESULTS

To show the reliability of the damage detection approach and also to survey the applicability of the proposed damage indicator, the acquired results of the HLBI are compared with those of technical literature[39]. For this purpose, a simply supported beam with a span length of l=0.6 (m) shown in Figure 2 is selected. The beam has a cross-section with dimensions of 0.02×0.04 m. The material density and modulus elasticity are $\rho = 7800\ \mathrm{kg/m^3}$ and $E = 206\ (GPa)$, respectively. The beam is discretized by 60 one-dimensional Euler-beam elements leading to 180 DOFs.

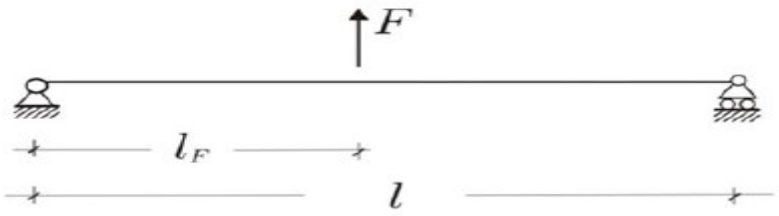

Fig. 2
The geometry of the simply supported beam under harmonic load[39].

As can be observed in Figures 3 to 5, the obtained results for different damage scenarios show a good match between the results of the proposed damage index under harmonic load and those of technical literature[39].

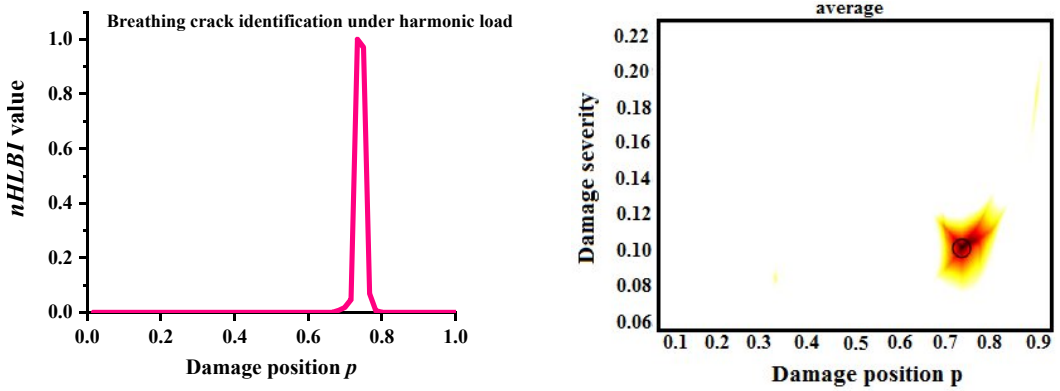

(a) This study (b) l_F/l=0.06; p = 0.73, s = 0.1 [39]

Fig. 3
Breathing crack identification on the simply supported beam under harmonic load: a) HLBI index b) proposed method by Casini et al. [39]

Where, l_F/l shows the position of the harmonic force and, p and s are the position and severity of the damage, respectively.

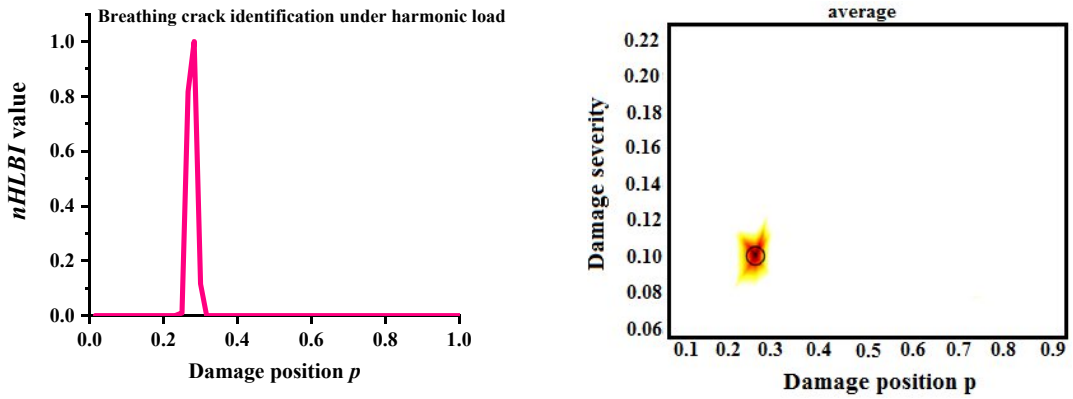

(a) This study (b)) l_F/l=0.06; p = 0.27, s = 0.1 Casini *et al*. [39]

Fig. 4
Breathing crack identification on the simply supported beam under harmonic load: a) HLBI index b) proposed method by Casini et al. [39].

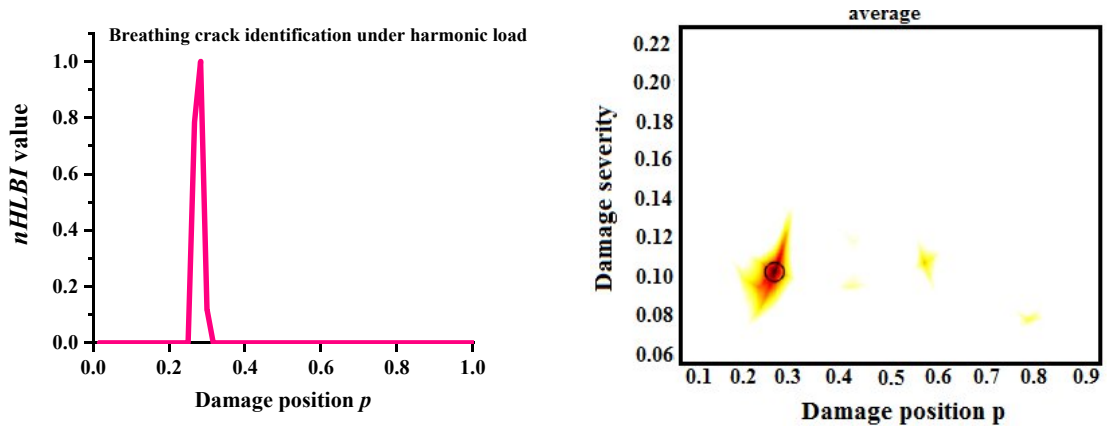

(a) This study (b)) l_F/l=0.45; p = 0.27, s = 0.1 Casini *et al*. [39]

Fig. 5
Breathing crack identification on the simply supported beam under harmonic load: a) HLBI index b) proposed method by Casini et al.[39] .

5. NUMERICAL EXAMPLES

To assess the applicability of the proposed method for detecting single and multiple damage scenarios, two examples are considered: a simply supported beam-column and a continues beam-column. The changes in various parameters that may affect the performance of the approach are studied. It's noted that in all damage scenarios, the moment of inertia (I) is reduced in damaged elements. Breathing cracks are considered in damaged elements, as described previously in section 3. The robustness of the proposed method in presence of damping and noise effects are also examined.

5.1. Example 1: A simply supported beam-column

A simply supported beam with a span length of L=5 (m) is selected as the first example (see Figure 6). Twenty elements and consequently sixty DOFs are considered for the beam. The beam has a cross-section of 0.2×0.2 m and an elasticity modulus of $E = 2.1\times10^{11}\ \mathrm{N/m^2}$. Table 1 shows 14 different damage scenarios under vertical (lateral) harmonic loading that are considered during the breathing cracks detection process. The effect of axial load is not considered in these 14 scenarios.

The first eighth scenario (cases 1-8) consists of a single crack. The ninth-fourteenth scenarios (cases 9-14) include multiple damage cases with different intensities. Also, cases 12 and 13 are introduced for considering the noise effects. In this example, 1.5 % noise is assumed in these scenarios. Moreover, the effect of changing in the direction of the transverse harmonic load and breathing cracks are examined in scenarios 1, 2, 5, and 6. It is worth mentioning that in all scenarios, the axial load is assumed to be zero. A MATLAB code using the Newmark-Beta method is prepared here for this purpose.

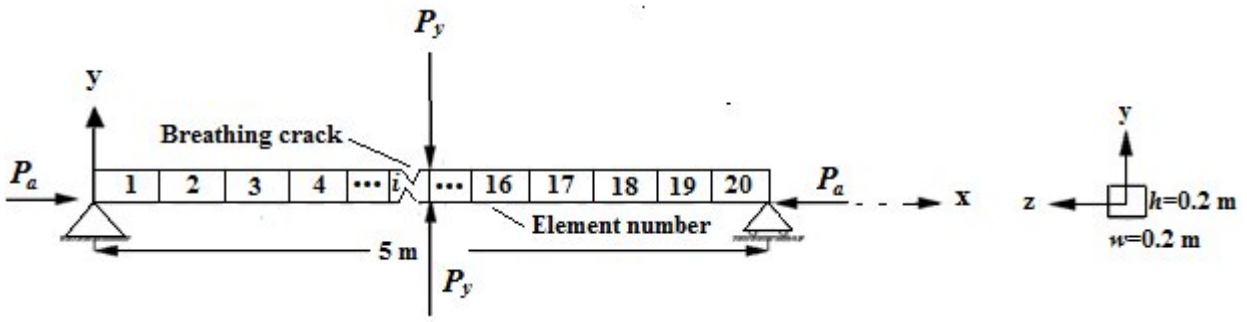

Fig. 6
(a) Geometry of the simply supported beam-column (b) Cross-section of the beam.

Table 1.
14 different damage scenarios induced in the simply supported beam

Case	Element number	Damage ratio[a] (%)	Damping ratio (ζ %)	P_v (KN) (vertical)	P_a (N) (axial)	Location of load (node)	noise (%)
1	1	10	0	-10×cos(*t*)[b]		11	0
2	1	10	0	10×cos(*t*)		11	0
3	2	10	0	-10×cos(*t*)		11	0
4	2	10	5	-10×cos(*t*)		11	0
5	6	15	0	-10×cos(*t*)		11	0
6	6	15	5	10×cos(*t*)		11	0
7	17	20	0	-10×cos(*t*)	0	11	0
8	17	20	5	-10×cos(*t*)		11	0
9	1 & 8	10	0	-10×cos(*t*)		11	0
10	1 & 8	10	5	-10×cos(*t*)		11	0
11	3 & 18	15	0	-10×cos(*t*)		11	0
12	3 & 18	15	5	-10×cos(*t*)		11	1.5
13	5 & 19	10 & 20	5	-10×cos(*t*)		11	1.5
14	2 & 10 & 18	20	5	-10×cos(*t*)		11	0

a Damage ratio is h_c/h where h_c is the crack depth
b $-1\le\cos(t)\le1$

The values of *nHLBI* for damage scenarios 1 to 14 are presented in Figure 7 (a)-(n), respectively.

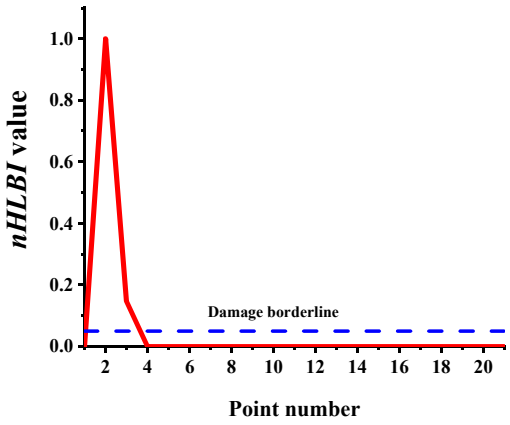

(a) Case-1

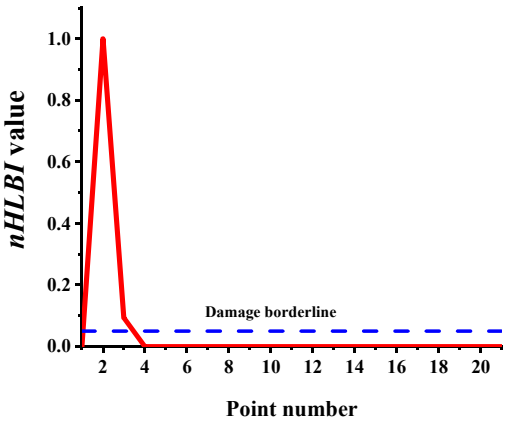

(b) Case-2

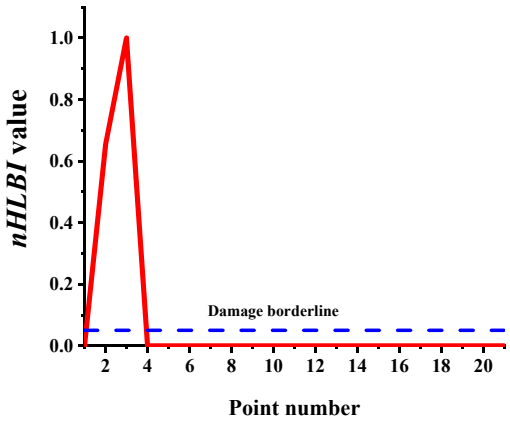

(c) Case-3

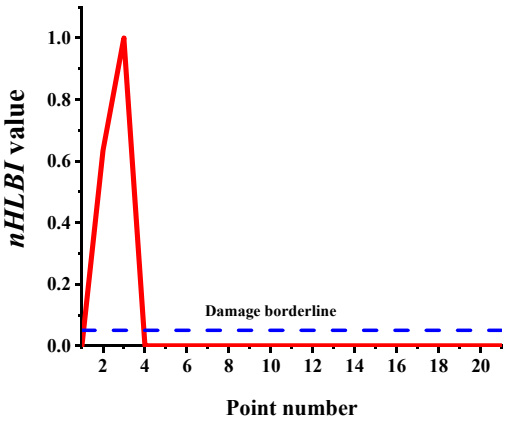

(d) Case-4

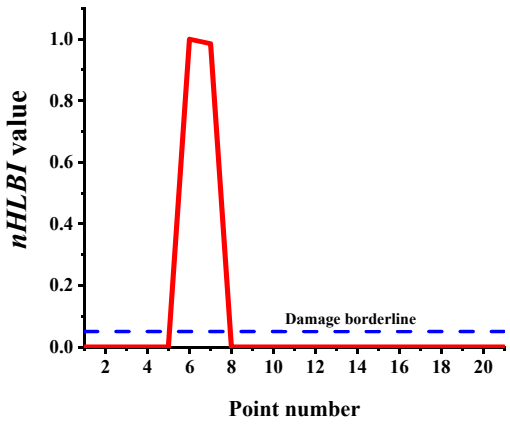

(e) Case-5

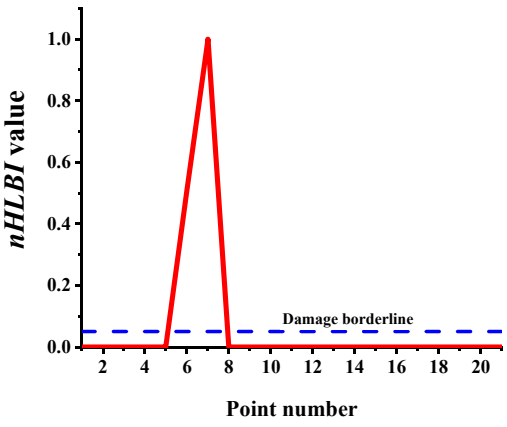

(f) Case-6

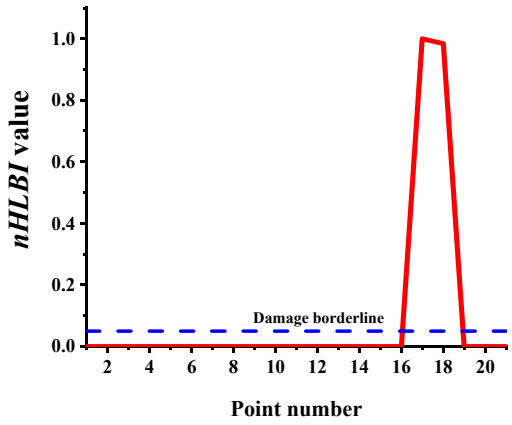

(g) Case-7

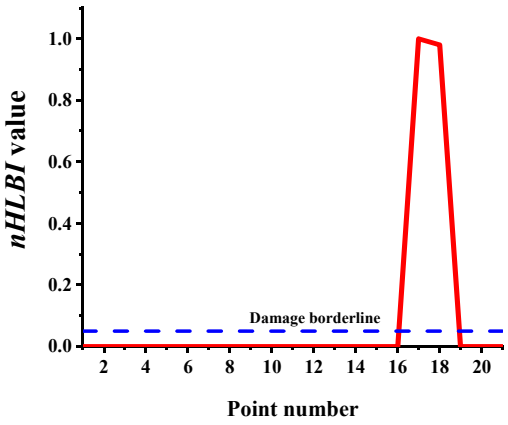

(h) Case-8

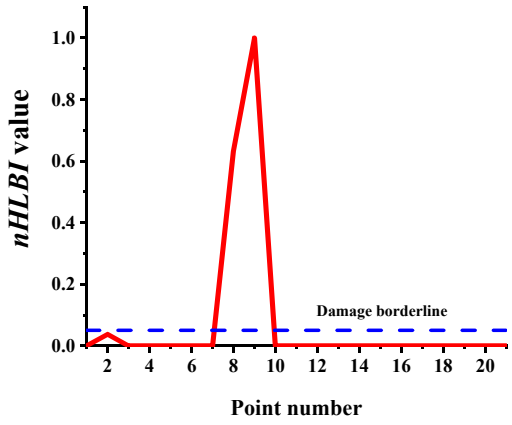

(i) Case-9

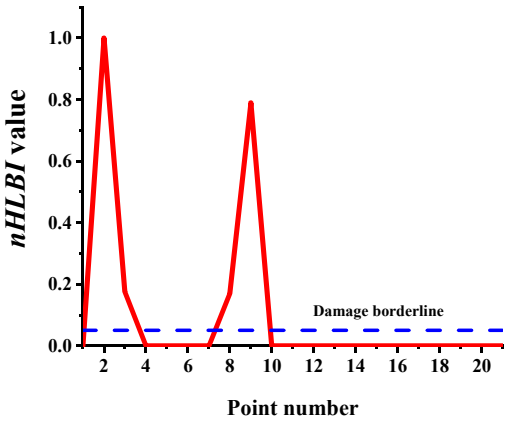

(j) Case-10

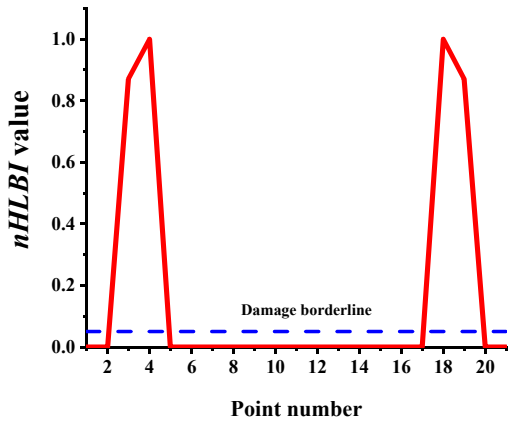

(k) Case-11

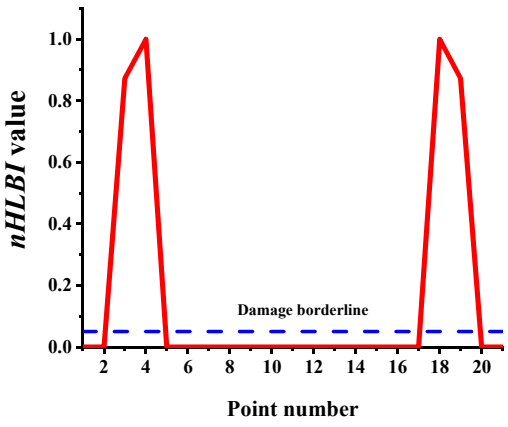

(l) Case-12

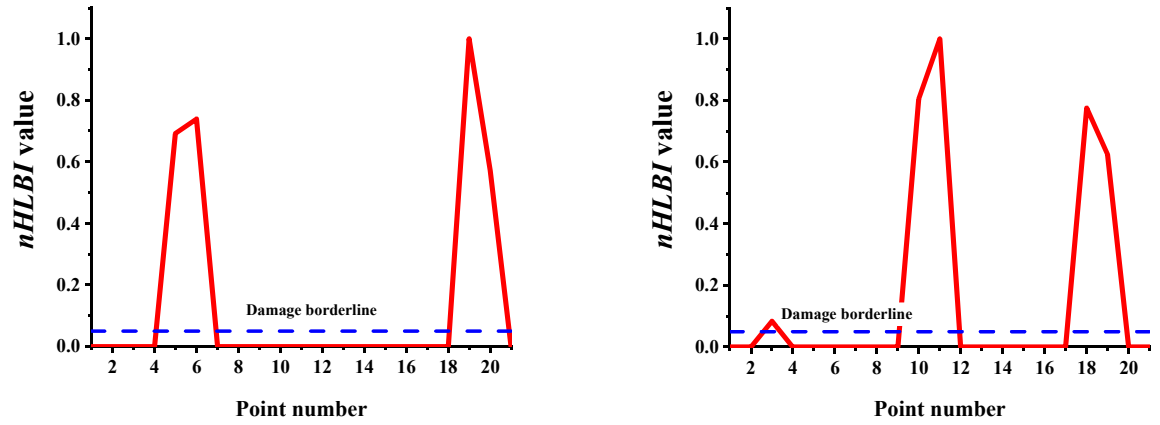

(m) Case-13 (n) Case-14

Fig. 7
Breathing crack identification of simply supported beam-column for cases 1-14.

As shown in the figures, the values of *nHLBI* are higher in the vicinity of some elements that indicate damage occurrence in these elements. A borderline value of 0.05 is considered for $nHLBI_{pi}$, and lower values are not considered during the damage detection process. Based on the defined threshold, it is revealed that the proposed index can accurately locate the single and multiple damage cases. Moreover, 1.5% noise is randomly applied in cases 12 and 13 on the response of the damaged structure.

The obtained results of Figures 7 (*l*) and 7(*m*) show the efficiency and capability of the *nHLBI*in diagnosing the breathing crack in the presence of noise effect. In other words, the noise has an approximately low effect on the performance of *nHLBI*. Moreover, the obtained results in Figures 7 (*i*) and (*j*) associated with cases 9 and 10 show a better performance of the crack detection approach in the presence of damping effects.

5.1.1. The axial load effects

As listed in Table 2, two damage cases, including six different axial loads (as a percentage of critical axial load), are considered to evaluate the axial load effect on the proposed approach and indictor. The results of case 1 for single crack and case 2 for multiple cracks are presented in Figures 8 and 9, respectively. Based on the results, the damage locations in single and multiple damage scenarios can be well detected in the presence of low axial loads. For higher axial load values (especially near critical axial load values), the structure may experience high deformations; in this situation, the modal responses and their derivatives are hugely affected by the axial load which may result in uncommon modal data (even in undamaged structure);In this case, the failure is practically occurred due to increasing the axial load in the cracked structural elements, and the common damage detection methods should not be applied for detection of the breathing crack damage. So, the numerical results of the proposed damage indicator are reasonable and show its reliable performance.

Table 2.
Different damage cases induced in simply supported beam-column including the axial load effect

Case 1			Case 2		
Element number	Damage ratio[a] (%)	Damping ratio (%)	Element number	Damage ratio[*] (%)	Damping ratio (%)
4	10	5	3	15	5
-	-	-	16	15	5
1	P_a=0.1P_{cr}			P_a=0.1P_{cr}	
2	P_a=0.3P_{cr}			P_a=0.3P_{cr}	
3	P_a=0.6P_{cr}			P_a=0.6P_{cr}	
4	P_a=0.8P_{cr}			P_a=0.8P_{cr}	
5	P_a=0.9P_{cr}			P_a=0.9P_{cr}	
6	P_a=0.989P_{cr}			P_a=0.986P_{cr}	

a Damage ratio is h_c/h where h_c is the crack depth

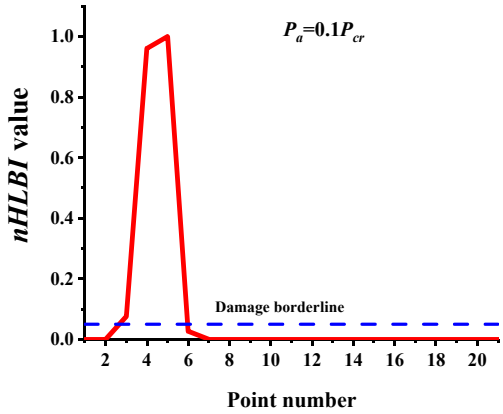

(a) Case 1-1

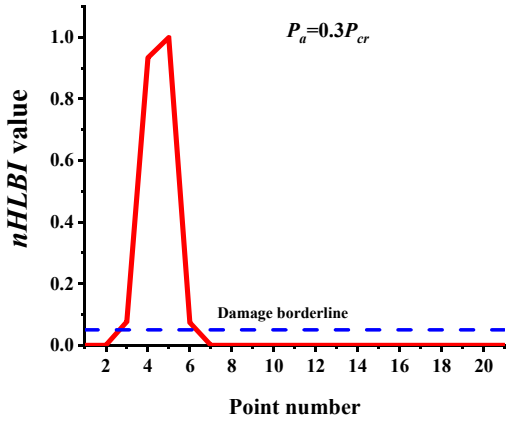

(b) Case 1-2

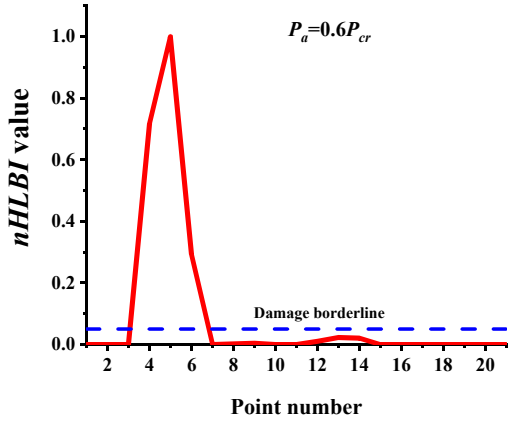

(c) Case 1-3

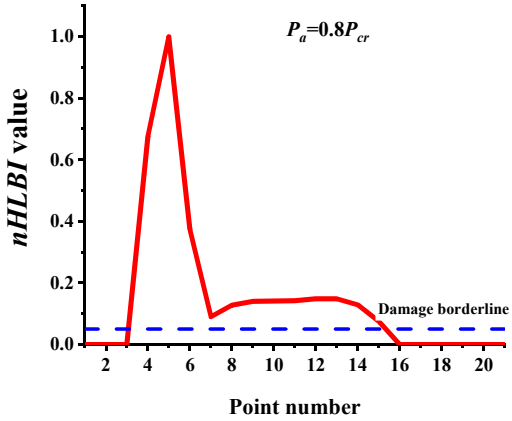

(d) Case 1-4

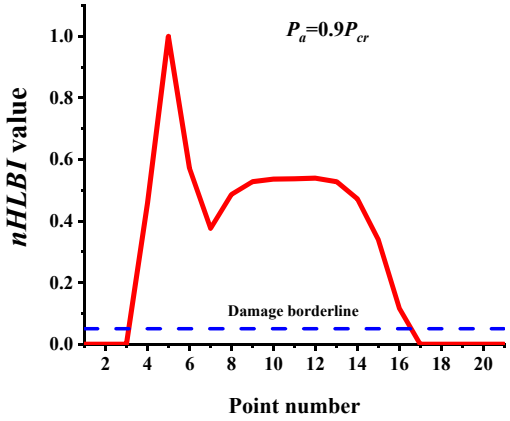

(e) Case 1-5

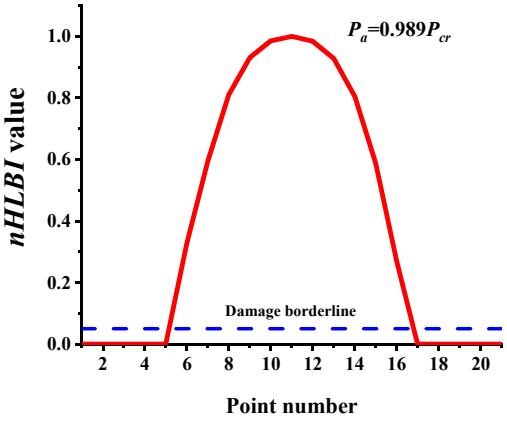

(f) Case 1-6

Fig. 8
Damage identification of simply supported beam-column for case 1 subjected to different axial loads.

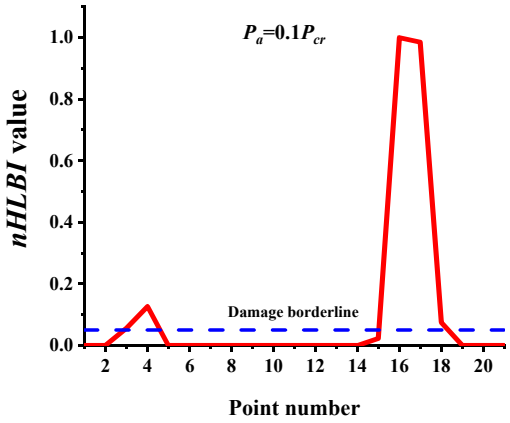

(a) Case 2-1

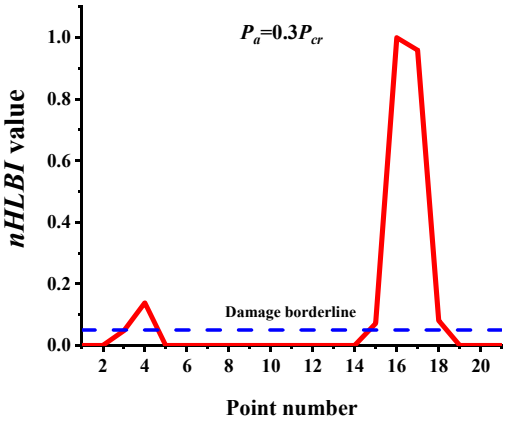

(b) Case 2-2

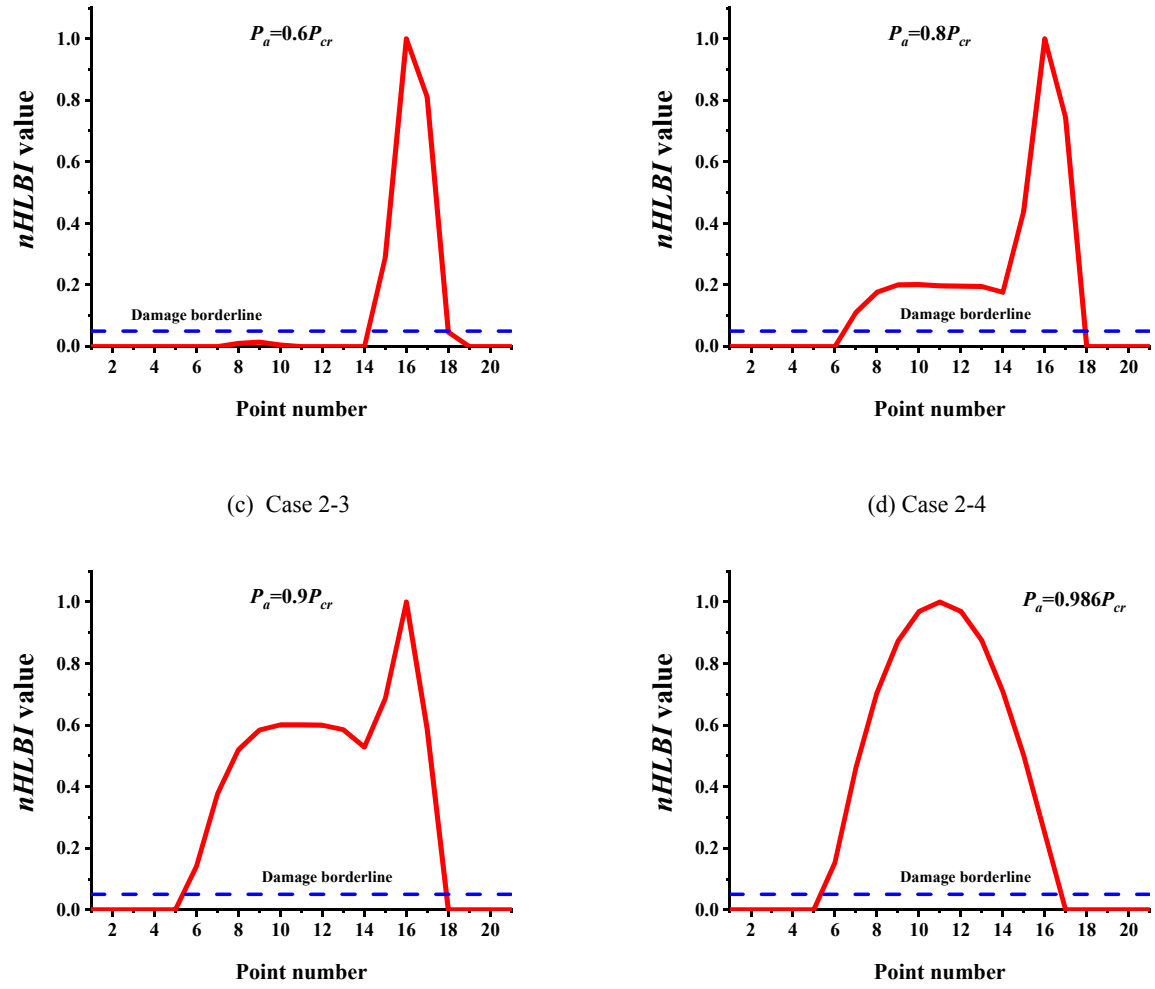

(c) Case 2-3

(d) Case 2-4

(e) Case 2-5

(f) Case 2-6

Fig. 9
Damage identification of simply supported beam-column for cases 2 subjected to different axial loads.

5.2. Example 2: A continues beam-column

A continuous beam-column with a span of L=5 (m) is selected as the second example (see Figure 10). The characteristics of the beam-column are similar to those of the first example. As shown in Table 3, for assessing the robustness of the proposed method, six different damage scenarios under vertical (lateral) harmonic loading are considered for detecting single and multiple breathing crack locations. In this example, the axial load is considered as $0.1P_{cr}$ for all six scenarios, and 1.5% random noise is assumed for scenario 5. A MATLAB code using the Newmark-Beta method is prepared here for this purpose.

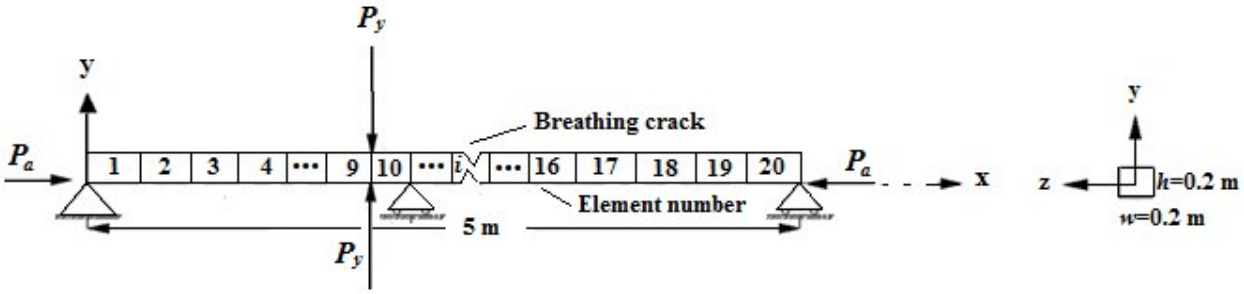

Fig. 10
(a) The geometry of the continuous beam-column (b) cross-section of the beam-column.

Table 3.
Six different damage scenarios induced in the continuous beam-column

Case	Element number	Damage ratio[a] (%)	Damping ratio (ζ %)	P_v (KN) (vertical)	P_a (N) (axial)	Location of load (node)	noise (%)
1	1	10	5	-10×cos(*t*)[b]		10	0
2	1	10	5	10×cos(*t*)		10	0
3	10	10	5	-10×cos(*t*)	$0.1P_{cr}$	10	0
4	2 & 15	10	5	10×cos(*t*)		10	0
5	9 & 19	10	5	-10×cos(*t*)		10	1.5
6	2, 10 & 18	10	5	-10×cos(*t*)		10	0

a Damage ratio is h_c/h where h_c is the crack depth
b $-1 \le \cos(t) \le 1$

Figure 11 shows the damage detection diagram of the continuous beam-column for cases 1 to 6, including different characteristics, which are listed in Table 3. As shown in the figure, the *nHLBI* can determine the cracked elements with high accuracy, applying both directions of the transverse harmonic load. Moreover, in case 5 with 1.5% random noise, the damaged elements are defined properly by the presented indicator, and an approximately negligible impact on the performance of *nHLBI* can be seen.

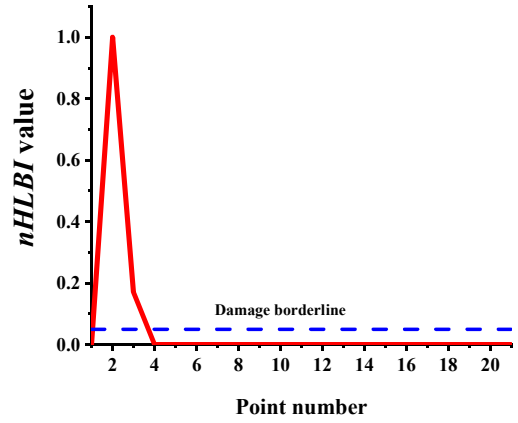

(a) Case-1

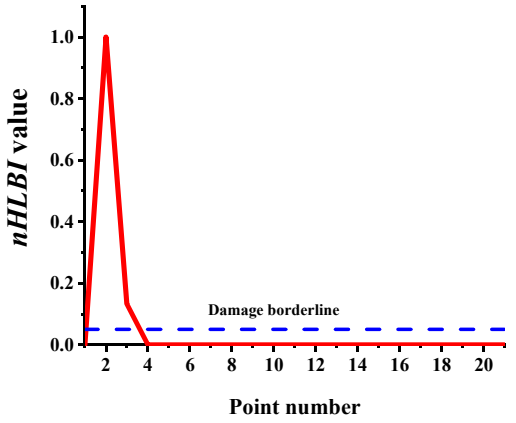

(b) Case-2

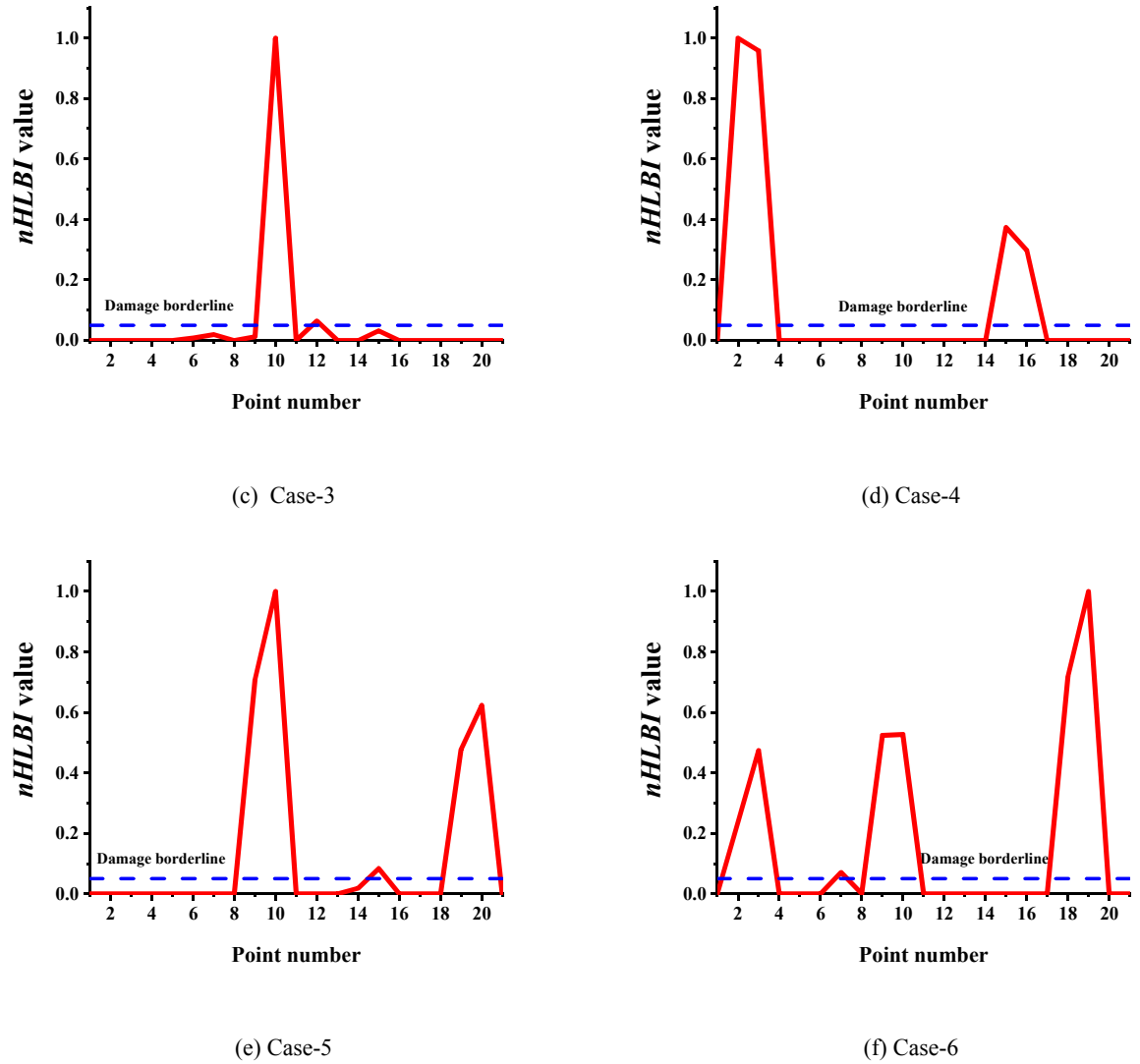

Fig. 11
Breathing crack identification of continuously supported beam-column for cases 1-6.

5.2.1 The axial load effect

As listed in Table 4, two illustrative damage scenarios, including six different axial loads (especially in the vicinity of critical load), are studied. As shown in Figures 12 and 13, the damage locations of single and multiple damage scenarios can be well defined in low axial loads. Similar to simply supported beam-column, in continuous beam-columns, increasing the axial load values (especially about the critical axial values), will result in a disturbance in the structural responses; the failure is practically occurred due to increasing the axial load in cracked elements, and consequently, the common damage detection approaches should not be used in this case. So, the results of the proposed damage indicator (*nHLBI*) are reasonable and show its reliable performance.

Table 4.
Different damage cases induced in continuous beam-column including the axial load effect

Case 1			Case 2		
Element number	Damage ratio[a] (%)	Damping ratio (%)	Element number	Damage ratio[a] (%)	Damping ratio (%)
5	10	5	3	10	5
-	-	-	16	10	5
1	P_a=0.1P_{cr}			P_a=0.1P_{cr}	
2	P_a=0.3P_{cr}			P_a=0.3P_{cr}	
3	P_a=0.6P_{cr}			P_a=0.6P_{cr}	
4	P_a=0.8P_{cr}			P_a=0.8P_{cr}	
5	P_a=0.9P_{cr}			P_a=0.9P_{cr}	
6	P_a=0.984P_{cr}			P_a=0.964P_{cr}	

a Damage ratio is h_c/h where h_c is the crack depth

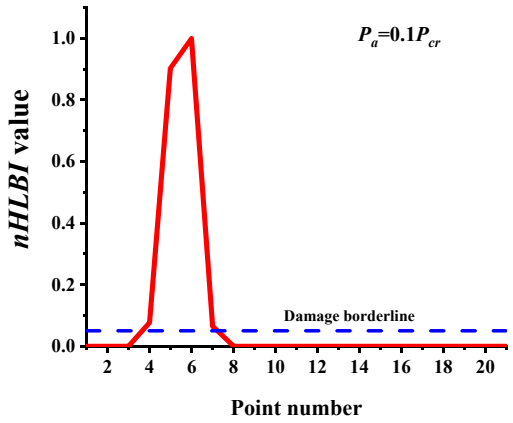

(a) Case 1-1

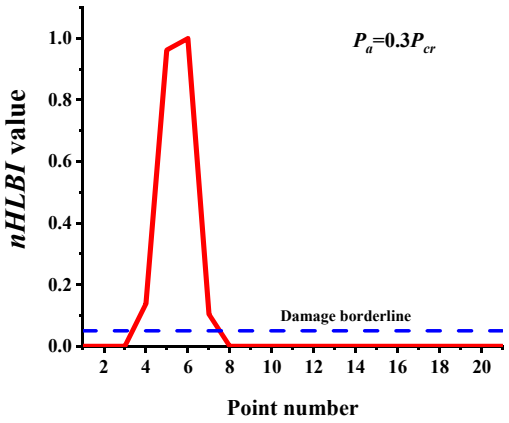

(b) Case 1-2

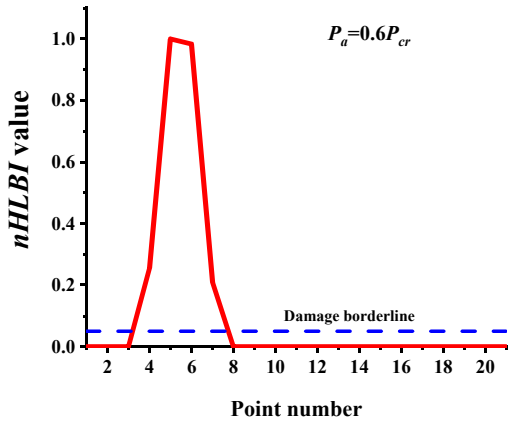

(c) Case 1-3

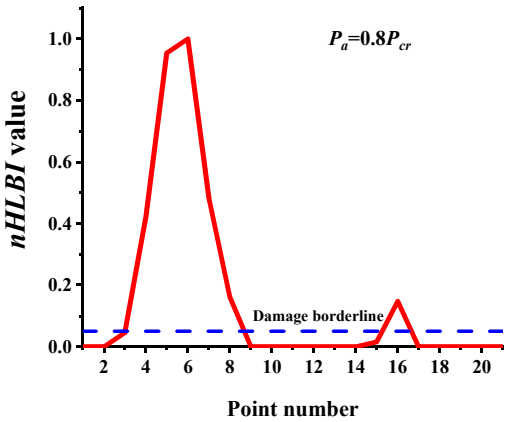

(d) Case 1-4

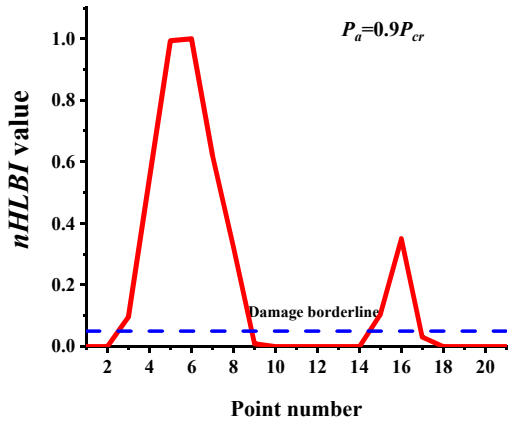

(e) Case 1-5

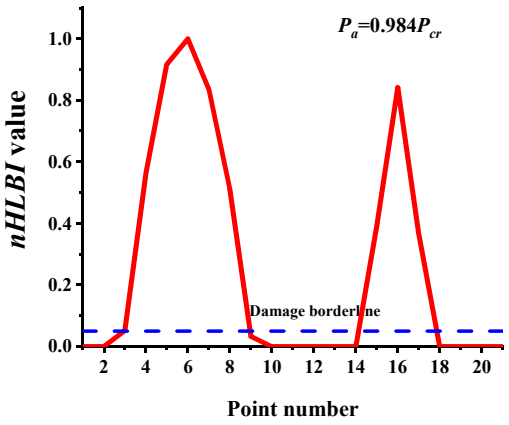

(f) Case 1-6

Fig. 12
Damage identification of continuous beam-column for case 1 subjected to different axial loads.

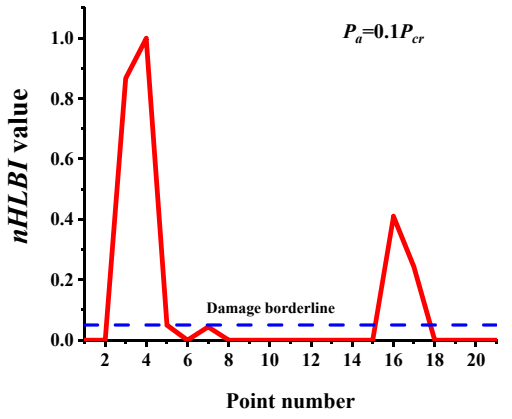

(a) Case 2-1

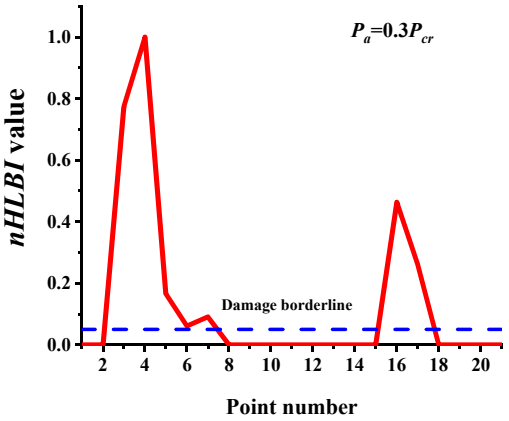

(b) Case 2-2

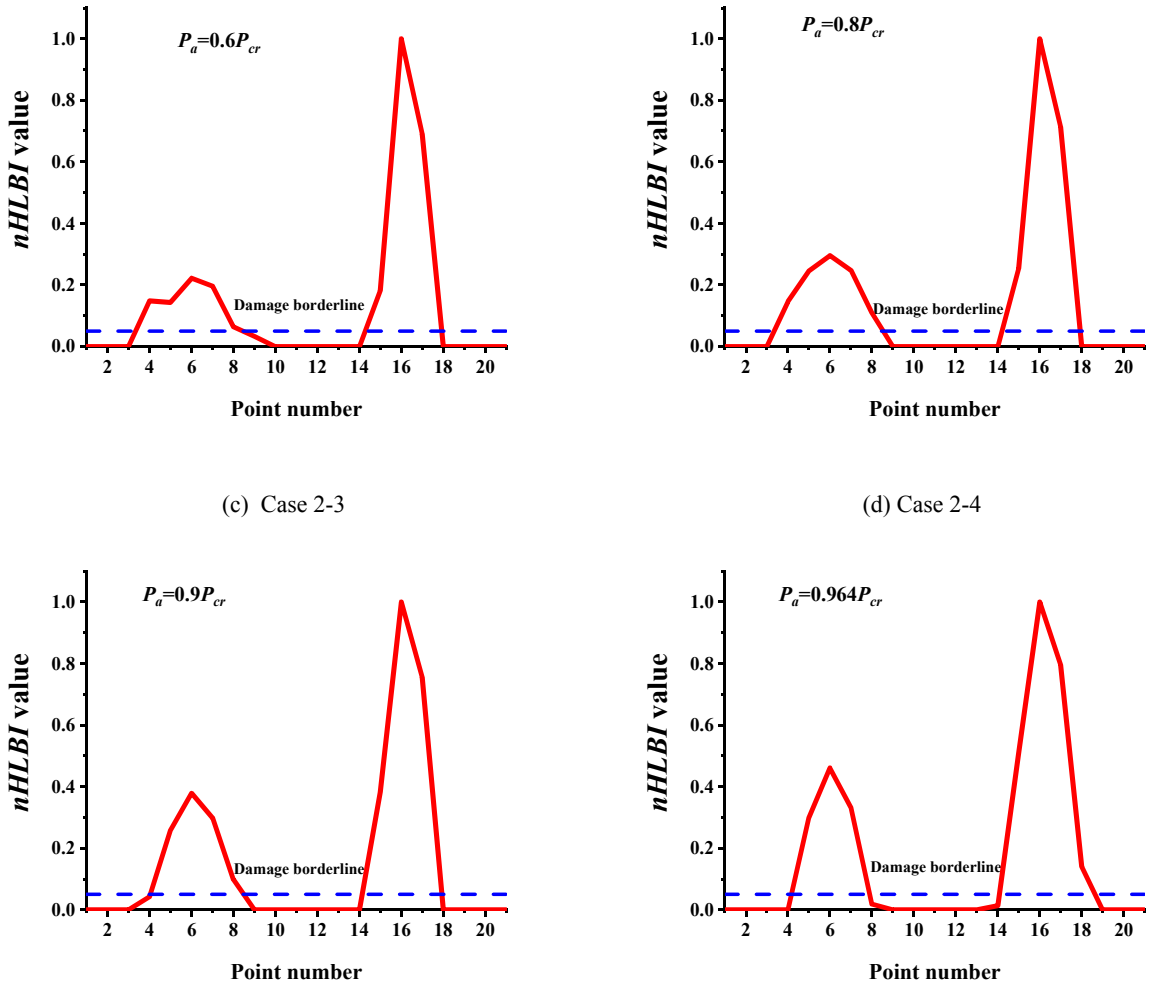

(c) Case 2-3

(d) Case 2-4

(e) Case 2-5

(f) Case 2-6

Fig. 13
Damage identification of continuous beam-column for case 2 subjected to different axial loads.

7. CONCLUSIONS

To assess the efficiency of the proposed method in diagnosing the breathing crack under harmonic load, different damage scenarios, including different characteristics, are investigated. The nonlinear behavior due to the presence of breathing crack is modeled using the Heaviside function to consider the bilinear stiffness behavior during open to close states. The effect of changes in the direction of harmonic load and also the noise and damping effect in the structural response is considered based on a proposed approach implemented on a MATLAB code using the Newmark-Beta method and a new damage indicator. The achievements based on the acquired results are listed as follows:

- The advantage of this study is breathing crack detection considering the axial load effects. The proposed method is accurately capable to detect the breathing crack location and leads to a better performance of the crack detection considering the damping effect in the dynamic equation of vibration.

- The results show that the presence of noise has an approximately negligible effect on the efficiency of the damage detection indicator.
- The beam-column structure in the vicinity of the critical load experiences high deformation. Failure in these cases practically is due to the increase of the axial load in the cracked elements. Therefore, the available damaged indicators without considering the slop term cannot be practically used anymore, while the proposed damage indicator is properly sensitive to this issue. Consequently, the results demonstrate that the proposed damage indicator and the presented damage approach lead to breathing crack detection with more accuracy in beam-column structures under harmonic loading.

REFERENCES

1. Adams R, Cawley P, Pye C, Stone B. A vibration technique for non-destructively assessing the integrity of structures. Journal of mechanical engineering science. 1978;20(2):93-100.
2. Rizos P, Aspragathos N, Dimarogonas A. Identification of crack location and magnitude in a cantilever beam from the vibration modes. Journal of sound and vibration. 1990;138(3):381-8.
3. Pandey A, Biswas M. Damage detection in structures using changes in flexibility. Journal of sound and vibration. 1994;169(1):3-17.
4. Capecchi D, Vestroni F. Monitoring of structural systems by using frequency data. Earthquake engineering & structural dynamics. 1999;28(5):447-61.
5. Vestroni F, Capecchi D. Damage detection in beam structures based on frequency measurements. Journal of engineering mechanics. 2000;126(7):761-8.
6. Seyedpoor S, Yazdanpanah O. An efficient indicator for structural damage localization using the change of strain energy based on static noisy data. Applied Mathematical Modelling. 2014;38(9-10):2661-72.
7. Chen H-P, Bicanic N. Assessment of damage in continuum structures based on incomplete modal information. Computers & structures. 2000;74(5):559-70.
8. Yazdanpanah O, Seyedpoor S, Akbarzadeh Bengar H. A new damage detection indicator for beams based on mode shape data. Structural Engineering and Mechanics. 2015;53(4):725-44.
9. Seyedpoor S, Yazdanpanah O. Structural damage detection by differential evolution as a global optimization algorithm. Iranian Journal of Structural Engineering. 2015;1(1):52-62.
10. Karimi S, Bozorgnsab M, Taghipour R, Alipour MM. A Novel Spring-Based Model for Damage Investigation of Functionally Graded Beams. Journal of Solid Mechanics. 2021:-.
11. Taghipour R, Nashta MR, Bozorgnasab M, Mirgolbabaei H. A new index for damage identification in beam structures based on modal parameters. Archive of Mechanical Engineering. 2021;68.
12. Pai PF, Young LG. Damage detection of beams using operational deflection shapes. International journal of solids and structures. 2001;38(18):3161-92.
13. Abdo M-B, Hori M. A numerical study of structural damage detection using changes in the rotation of mode shapes. Journal of Sound and vibration. 2002;251(2):227-39.
14. Shih HW, Thambiratnam D, Chan T. Vibration based structural damage detection in flexural members using multi-criteria approach. Journal of sound and vibration. 2009;323(3-5):645-61.
15. Navabian N, Bozorgnasab M, Taghipour R, Yazdanpanah O. Damage identification in plate-like structure using mode shape derivatives. Archive of Applied Mechanics. 2016;86(5):819-30.
16. Navabian N, Taghipour R, Bozorgnasab M, Ghasemi J. Damage evaluation in plates using modal data and firefly optimisation algorithm. International Journal of Structural Engineering. 2018;9(1):50-69.
17. Moradi S, Razi P, Fatahi L. On the application of bees algorithm to the problem of crack detection of beam-type structures. Computers & Structures. 2011;89(23-24):2169-75.
18. Nobahari M, Seyedpoor SM. An efficient method for structural damage localization based on the concepts of flexibility matrix and strain energy of a structure. Structural Engineering and Mechanics. 2013;46(2):231-44.
19. Yazdanpanah O, Izadifard RA, Dehestani M. Static data based damage localization of beam-column structures considering axial load. Mechanics of Advanced Materials and Structures. 2020;27(16):1433-50.
20. Roodgar Nashta M, Taghipour R, Bozorgnasab M, Mirgolbabaei M. A novel method for identification of damage location in frame structures using a modal parameters-based indicator .Archives of Civil Engineering.2022; 68(3):633-643.
21. Ruotolo R, Surace C, Crespo P, Storer D. Harmonic analysis of the vibrations of a cantilevered beam with a closing crack. Computers & structures. 1996;61(6):1057-74.
22. Pugno N, Ruotolo R, Surace C. Analysis of the harmonic vibrations of a beam with a breathing crack. Proc 15th IMAC (Tokyo, Japan). 1997:409-13.

23. Tsyfansky S, Beresnevich V. Detection of fatigue cracks in flexible geometrically non-linear bars by vibration monitoring. Journal of Sound and vibration. 1998;213(1):159-68.
24. Tsyfansky SL, Beresnevich V. Non-linear vibration method for detection of fatigue cracks in aircraft wings. Journal of sound and vibration. 2000;236(1):49-60.
25. Guo C, Al-Shudeifat M, Yan J, Bergman L, McFarland D, Butcher E. Application of empirical mode decomposition to a Jeffcott rotor with a breathing crack. Journal of Sound and Vibration. 2013;332(16):3881-92.
26. Saavedra P, Cuitino L. Crack detection and vibration behavior of cracked beams. Computers & Structures. 2001;79(16):1451-9.
27. Bovsunovsky A, Surace C, Ruotolo R, editors. The effect of damping on the non-linear dynamic behaviour of a cracked beam at resonance and super-resonance vibrations. Key Engineering Materials; 2003: Trans Tech Publ.
28. Al-Shudeifat MA, Butcher EA. New breathing functions for the transverse breathing crack of the cracked rotor system: approach for critical and subcritical harmonic analysis. Journal of Sound and Vibration. 2011;330(3):526-44.
29. Liu W, Barkey ME. The effects of breathing behaviour on crack growth of a vibrating beam. Shock and Vibration. 2018;2018.
30. Bovsunovsky AP, Surace C. Considerations regarding superharmonic vibrations of a cracked beam and the variation in damping caused by the presence of the crack. Journal of Sound and Vibration. 2005;288(4-5):865-86.
31. Chatterjee A. Structural damage assessment in a cantilever beam with a breathing crack using higher order frequency response functions. Journal of Sound and Vibration. 2010;329(16):3325-34.
32. Joglekar D, Mitra M. Analysis of flexural wave propagation through beams with a breathing crack using wavelet spectral finite element method. Mechanical Systems and Signal Processing. 2016;76:576-91.
33. Prawin J, Lakshmi K, Rao ARM. A novel singular spectrum analysis–based baseline-free approach for fatigue-breathing crack identification. Journal of Intelligent Material Systems and Structures. 2018;29(10):2249-66.
34. Shariyat, M., Alipour, M.M. Differential transform vibration and modal stress analyses of circular plates made of two-directional functionally graded materials resting on elastic foundations. Arch Appl Mech 81, 1289–1306 (2011).
35. Chu Y, Shen M-H. Analysis of forced bilinear oscillators and the application to cracked beam dynamics. AIAA journal. 1992;30(10):2512-9.
36. Casini P, Vestroni F. Characterization of bifurcating non-linear normal modes in piecewise linear mechanical systems. International Journal of Non-Linear Mechanics. 2011;46(1):142-50.
37. Chati M, Rand R, Mukherjee S. Modal analysis of a cracked beam. Journal of sound and vibration. 1997;207(2):249-70.
38. Yoo CH, Lee S. Stability of structures: principles and applications: Elsevier; 2011.
39. Casini P, Vestroni F, Giannini O. Crack detection in beam-like structures by nonlinear harmonic identification. Frattura ed Integrità Strutturale. 2014;8(29):313-24.
40. Benfratello S, Cacciola P, Impollonia N, Masnata A, Muscolino G. Numerical and experimental verification of a technique for locating a fatigue crack on beams vibrating under Gaussian excitation. Engineering Fracture Mechanics. 2007;74(18):2992-3001.
41. Zareian F, Medina RA. A practical method for proper modeling of structural damping in inelastic plane structural systems. Computers & structures. 2010;88(1-2):45-53.
42. Haselton CB, Liel AB, Deierlein GG, Dean BS, Chou JH. Seismic collapse safety of reinforced concrete buildings. I: Assessment of ductile moment frames. Journal of Structural Engineering. 2011;137(4):481-91.
43. Chopra AK. Dynamics of structures. Theory and Application to Earthquake Engineering: Prentice Hall, New Jersey; 1995.
44. Chowdhury I, Dasgupta SP. Computation of Rayleigh damping coefficients for large systems. The Electronic Journal of Geotechnical Engineering. 2003;8(0):1-11.
45. Song Z, Su C. Computation of Rayleigh damping coefficients for the seismic analysis of a hydro-powerhouse. Shock and Vibration. 2017;2017.
46. Gavin H. Numerical integration for structural dynamics. Department of Civil and Environmental Engineering, Duke University: Durham, NC, USA2001.
47. Zhou X, Sha D, Tamma KK. A novel non□linearly explicit second□order accurate L□stable methodology for finite deformation: hypoelastic/hypoelasto□plastic structural dynamics problems. International Journal for Numerical Methods in Engineering. 2004;59(6):795-823.
48. Soroushian A, editor On practical performance of a technique recently proposed for time integration analysis with less computational cost. Proceedings of the 17th International Congress on Sound & Vibration; 2010.
49. Nateghi F, Yakhchalian M, editors. On less computational costs for analysis of silos seismic behaviors by time integration. Proceedings of the 3rd ECCOMAS thematic conference on computational methods in structural dynamics and earthquake engineering (COMPDYN 2011), Corfu; 2011.
50. MATLAB M. Statistics and Machine Learning Toolbox: 2017a–Ensemble Methods. The MathWorks Inc, Natick, Massachusetts, United States. 2017.